

## Optimizing direct magnetoelectric coupling in Pb(Zr,Ti)O<sub>3</sub>/Ni multiferroic film heterostructures

Ming Feng, Jian-jun Wang, Jia-Mian Hu, Jing Wang, Jing Ma, Hai-Bo Li, Yang Shen, Yuan-Hua Lin, Long-Qing Chen, and Ce-Wen Nan

Citation: *Applied Physics Letters* **106**, 072901 (2015); doi: 10.1063/1.4913471

View online: <http://dx.doi.org/10.1063/1.4913471>

View Table of Contents: <http://scitation.aip.org/content/aip/journal/apl/106/7?ver=pdfcov>

Published by the [AIP Publishing](#)

---

### Articles you may be interested in

[Converse magnetoelectric coupling in NiFe/Pb\(Mg<sub>1/3</sub>Nb<sub>2/3</sub>\)O<sub>3</sub>-PbTiO<sub>3</sub> nanocomposite thin films grown on Si substrates](#)

*Appl. Phys. Lett.* **103**, 192903 (2013); 10.1063/1.4828878

[Large remanent polarization in multiferroic NdFeO<sub>3</sub>-PbTiO<sub>3</sub> thin film](#)

*Appl. Phys. Lett.* **103**, 082904 (2013); 10.1063/1.4819386

[Low moment NiCr radio frequency magnetic films for multiferroic heterostructures with strong magnetoelectric coupling](#)

*J. Appl. Phys.* **111**, 103915 (2012); 10.1063/1.4722344

[Residual stress and magnetic behavior of multiferroic CoFe<sub>2</sub>O<sub>4</sub>/Pb\(Zr<sub>0.52</sub>Ti<sub>0.48</sub>\)O<sub>3</sub> thin films](#)

*J. Appl. Phys.* **105**, 084113 (2009); 10.1063/1.3115452

[Evaluation of magnetoelectric coupling in a BaTiO<sub>3</sub>-Ni composite ferroic film by impedance spectroscopy](#)

*Appl. Phys. Lett.* **92**, 214101 (2008); 10.1063/1.2920809

---



You don't still use this cell phone



or this computer



Why are you still using an AFM designed in the 80's?



**It is time to upgrade your AFM**  
Minimum \$20,000 trade-in discount for purchases before August 31st

Asylum Research is today's technology leader in AFM

[dropmyoldAFM@oxinst.com](mailto:dropmyoldAFM@oxinst.com)



**OXFORD**  
INSTRUMENTS  
*The Business of Science®*

## Optimizing direct magnetoelectric coupling in Pb(Zr,Ti)O<sub>3</sub>/Ni multiferroic film heterostructures

Ming Feng,<sup>1,2,a)</sup> Jian-jun Wang,<sup>1,3,a,b)</sup> Jia-Mian Hu,<sup>3</sup> Jing Wang,<sup>4</sup> Jing Ma,<sup>1</sup> Hai-Bo Li,<sup>2</sup> Yang Shen,<sup>1</sup> Yuan-Hua Lin,<sup>1</sup> Long-Qing Chen,<sup>1,3</sup> and Ce-Wen Nan<sup>1,b)</sup>

<sup>1</sup>State Key Lab of New Ceramics and Fine Processing, School of Materials Science and Engineering, Tsinghua University, Beijing 100084, China

<sup>2</sup>Key Laboratory of Functional Materials Physics and Chemistry of the Ministry of Education, Jilin Normal University, Changchun 130103, China

<sup>3</sup>Department of Materials Science and Engineering, The Pennsylvania State University, University Park, Pennsylvania 16802, USA

<sup>4</sup>State Key Laboratory of Mechanics and Control of Mechanical Structures, and College of Aerospace Engineering, Nanjing University of Aeronautics and Astronautics, Nanjing 210016, People's Republic of China

(Received 31 December 2014; accepted 11 February 2015; published online 19 February 2015)

Polycrystalline Pt thin films of different thicknesses (0–75 nm) were introduced using magnetron sputtering in Pb(Zr<sub>0.52</sub>Ti<sub>0.48</sub>)O<sub>3</sub> (PZT, 400 nm in thickness)/Pt/Ni multiferroic film heterostructures, aimed at optimizing the transfer efficiency of magnetostrictive strain from the bottom Ni foil to the top PZT film and thus the direct magnetoelectric (ME) coupling. The ME voltage coefficient  $\alpha_{E31}$  was directly measured, while the strain transfer efficiency  $k$  was obtained by combined experimental and theoretical analysis. At the optimum Pt-thickness of 30 nm, the polycrystalline film heterostructure shows the largest  $\alpha_{E31}$  of 772 mV cm<sup>-1</sup> Oe<sup>-1</sup> at a low dc magnetic bias field of 86 Oe, as well as the highest  $k$  of 83% that is comparable to that in epitaxial quasi-2-2 film heterostructures. © 2015 AIP Publishing LLC. [<http://dx.doi.org/10.1063/1.4913471>]

Strong direct magnetoelectric (ME) couplings, i.e., magnetic-field-induced polarization or voltage output, have been demonstrated at room temperature via magneto-mechanical-electric cross coupling in multiferroic piezoelectric/magnetostrictive composites,<sup>1–3</sup> which has enabled several smart device designs such as highly sensitive magnetic-field sensors,<sup>4–7</sup> low-power read heads for magnetic hard disks,<sup>8</sup> and magnetic energy harvesters.<sup>9</sup> Among them, layered piezoelectric/magnetostrictive composite structures are most attractive. The layered bulk composites were usually fabricated by either co-firing two oxide phases (i.e., piezoelectric oxides and ferrites) at high temperatures (normally over 1200 °C) or bonding the magnetic and piezoelectric phases together using organic binders. However, atomic interdiffusion and reaction cross the interface between the two oxide phases unavoidably occur during the high-temperature processing; and due to the thermal expansion mismatch, micro-cracks may also appear. Both of these, as well as the interfacial organic binder layer, would greatly deteriorate the ME coupling, especially the long-term stability.<sup>10</sup>

Recent progress in enhancing the ME response of layered multiferroic film heterostructures, in which the substrate-imposed clamping on magnetostrictive deformation (strain) has been relieved by introducing thin cantilever substrates,<sup>11–14</sup> greatly facilitates the on-chip integration of these smart ME devices. An alternative to relieve such substrate clamping is to directly grow the piezoelectric thin film on a magnetostrictive substrate, known as a quasi-2–2 multiferroic film heterostructures,<sup>1</sup> which has an even simpler

structure and allows highly efficient transfer of magnetostrictive strain across interface. For example, a high ME voltage coefficient of 600 mV cm<sup>-1</sup> Oe<sup>-1</sup> has been observed at low temperature of 120 K in an epitaxial Pb(Zr,Ti)O<sub>3</sub> (PZT) film directly grown on a La<sub>1.2</sub>Sr<sub>1.8</sub>Mn<sub>2</sub>O<sub>7</sub> single crystal, which is about 87% of the theoretical value assuming zero loss of strain.<sup>15</sup> Nevertheless, in a polycrystalline PZT film spin-coated on a dense CoFe<sub>2</sub>O<sub>4</sub> ceramic plate, the ME voltage coefficient observed at room temperature is only about 60 mV cm<sup>-1</sup> Oe<sup>-1</sup>, much less than the theoretical estimation;<sup>17</sup> and can be increased to 155 mV cm<sup>-1</sup> Oe<sup>-1</sup> when introducing LaNiO<sub>3</sub> film as electrode and buffer layer sandwiched between the PZT film and CoFe<sub>2</sub>O<sub>4</sub> ceramic plate.<sup>18</sup> Thus, the interfacial bonding layer still plays a key role in achieving strong direct ME coupling in such simple quasi-2–2 film heterostructures.

In order to achieve strong ME coupling at both low field and room temperature, grow the piezoelectric oxide thin film (e.g., PZT) directly onto a soft magnetic metal or alloy rather than a magnetic oxide as discussed above has been highly desired. However, the interface control is challenging due to big difference between PZT and soft metallic magnet. In this work, we report the PZT film directly growing onto a soft magnet Ni foil by controlling the interfacial bonding layer. A Pt buffer layer was introduced to achieve structurally more coherent hetero-interface because of its intermediate lattice constant (i.e., 3.912 Å for cubic Pt) between cubic PZT (4.036 Å) and face-centered cubic Ni (3.54 Å), aiming at improving the transfer efficiency of magnetostrictive strain across the interface. Obviously, the Pt layer would play a key role in the direct magneto-electric effect of the film heterostructures. The present results clearly demonstrate

<sup>a)</sup>Ming Feng and Jian-jun Wang contributed equally to this work.

<sup>b)</sup>Authors to whom correspondence should be addressed. Electronic addresses: wjj8384@gmail.com and cwnan@tsinghua.edu.cn

how the Pt buffer layer affects the strain transfer efficiency and hence the ME voltage output.

Heterostructures of PZT/Pt thin films were grown on the 0.2-mm-thick polycrystalline Ni foil by a combination of off-axis magnetron sputtering (Pt) and sol-gel spin-coating technique (PZT). First, for the preparation of the PZT/Pt bilayered films, the Pt films were sputtered on the Ni foil using the off-axis magnetron sputtering at 200 °C. The thickness of Pt layer was controlled by the sputtering time. Before deposition, the sputtering chamber was vacuumed to a base pressure of  $1 \times 10^{-7}$  Torr. A power of 40 W and Ar gas pressure of  $2 \times 10^{-3}$  Torr were used for the deposition of Pt. Second, the PZT films were grown on Pt films via a simple sol-gel spin-coating method as before. The PZT precursor solutions were spin coated on the Pt/Ni substrate at 3500 rpm for 30 s and pyrolyzed on a hot foil at 400 °C for 5 min. The pyrolyzed thin films were performed by repeating above processes to obtain a desired thickness, and finally annealed at 650 °C for 10 min in air. For electrical measurements, top Pt dot electrodes of about 300  $\mu\text{m}$  in diameter were deposited on the PZT film by magnetron sputtering.

Fig. 1(a) shows the X-ray diffraction (XRD) patterns of the PZT(400 nm)/Pt/Ni film heterostructures with the thickness of Pt buffer layer varying from 0 nm to 75 nm. These thickness values are obtained from cross-sectional SEM images (e.g., see Fig. 1(b)). As shown in Fig. 1(a), a (200)-oriented NiO impurity phase, originates during the PZT annealing in air,<sup>19</sup> is found at  $2\theta = 43.6^\circ$  for all samples. Both Ni and PZT are polycrystalline evidenced by their multiple peaks observed in the XRD pattern. For samples without and with different thickness of Pt buffer layers, the PZT films show nearly the same XRD patterns, indicating that the Pt buffer layer has ignorable effect on the PZT film crystallinity. The cross-sectional SEM images indicate that the interfacial connections of PZT-Pt and Pt-Ni are in good quality. Moreover, the PZT film shows a dense polygrain structure with grain size ranging from 80 nm to 250 nm, as shown from its surface morphology in Fig. 1(c).

Well-defined and symmetric ferroelectric hysteresis loops are obtained under electric fields applied perpendicular to the surface of the quasi-2-2 PZT/Pt/Ni film heterostructures. As shown in Fig. 2(a), with thickness of the Pt buffer layer ranging from 0 nm to 75 nm, the ferroelectric hysteresis loops are very similar, especially characterized by nearly the same coercive fields. All the PZT films get fully polarized at about 250 kV/cm with corresponding saturation polarizations  $P_s$  about 60  $\mu\text{C}/\text{cm}^2$ . The remnant polarizations  $P_r$  for all samples are about 30  $\mu\text{C}/\text{cm}^2$ , which is comparable to those PZT films grown on Si substrate with Pt ( $\sim 30 \mu\text{C}/\text{cm}^2$ ),<sup>20</sup>  $\text{La}_{0.5}\text{Sr}_{0.5}\text{CoO}_3$  ( $\sim 20 \mu\text{C}/\text{cm}^2$ ),<sup>21</sup>  $\text{LaNiO}_3$  ( $17 \sim 20 \mu\text{C}/\text{cm}^2$ ),<sup>22</sup> or  $\text{SrTiO}_3$  ( $25 \sim 40 \mu\text{C}/\text{cm}^2$ )<sup>23</sup> as the buffer layers, respectively. Fig. 2(b) shows the frequency-dependent dielectric constant and loss which indicates  $\epsilon_{33}^p$  of about 1178 for the PZT film at low frequency (100 Hz) with low dielectric loss (i.e., below 0.03 for most frequencies). Fig. 2(c) presents the typical butterfly-shaped piezoelectric strain loop of the PZT film, from which the piezoelectric coefficient  $d_{33}^p$  can be defined by taking the slope of the strain at each applied electric field to the origin ( $d_{33}^p = \Delta\eta_{33}/\Delta E_3$ ).<sup>24</sup> As exhibited in Fig. 2(c), a portion of the strain loop (from A to B in red

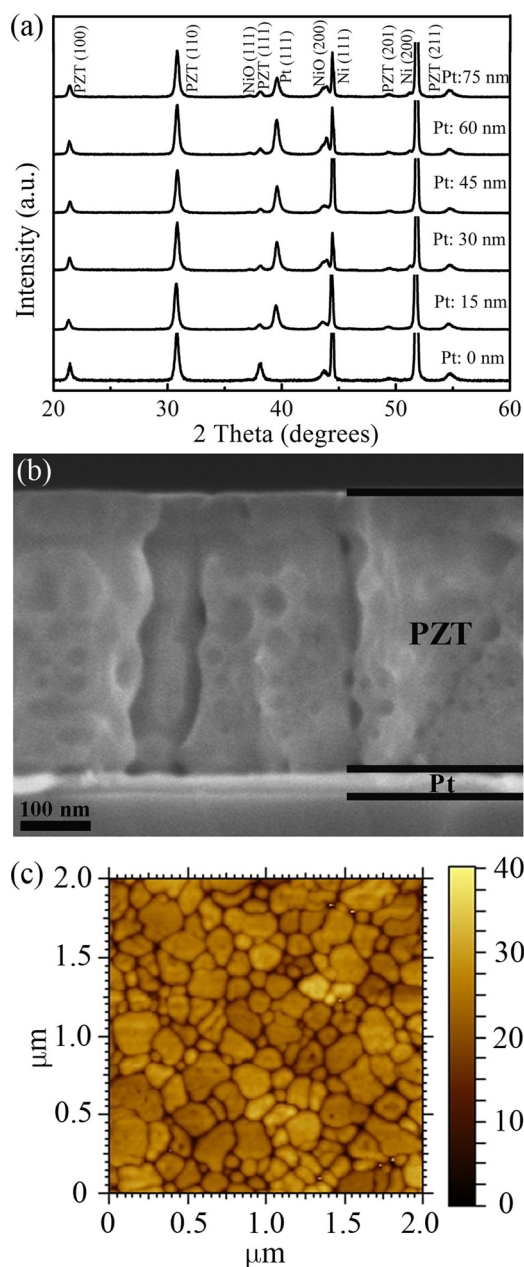


FIG. 1. Structures and morphologies of the PZT/Pt/Ni heterostructure: (a) XRD pattern of the PZT/Pt/Ni film heterostructures with different thickness of Pt buffer layers; (b) SEM image for the cross-section of PZT and Pt layers; and (c) two-dimensional AFM image (top view) of the PZT film.

color) is used to extract  $d_{33}$  (85 ~ 150 pm/V) as function of strain  $\eta_{33}$  (see the top inset of Fig. 2(c)). As shown in the bottom inset of Fig. 2(c), the similarity of the  $\eta_{33}$  versus  $E_3$  loops indicates that of Pt buffer layer has no significant effect on the piezoelectricity of the PZT films. Therefore, the good performances of the ferroelectric, dielectric, and piezoelectric behaviors indicate that the PZT films were well grown on Ni foil without or with different thickness of Pt as the buffer layers.

Fig. 3(a) shows the magnetostrictive properties of the Ni foil that exhibits a saturation in-plane magnetostrictive strain  $\lambda$  of  $-34$  ppm under a static in-plane magnetic field  $H_1^{\text{dc}}$  of 250 Oe. Particularly, a maximum piezomagnetic coefficient  $d\lambda/dH_1^{\text{dc}}$  of  $-0.2$  ppm/Oe is exhibited at  $H_1^{\text{dc}} = 86$  Oe, much larger than the  $-0.04$  ppm/Oe in CFO ceramics at similar

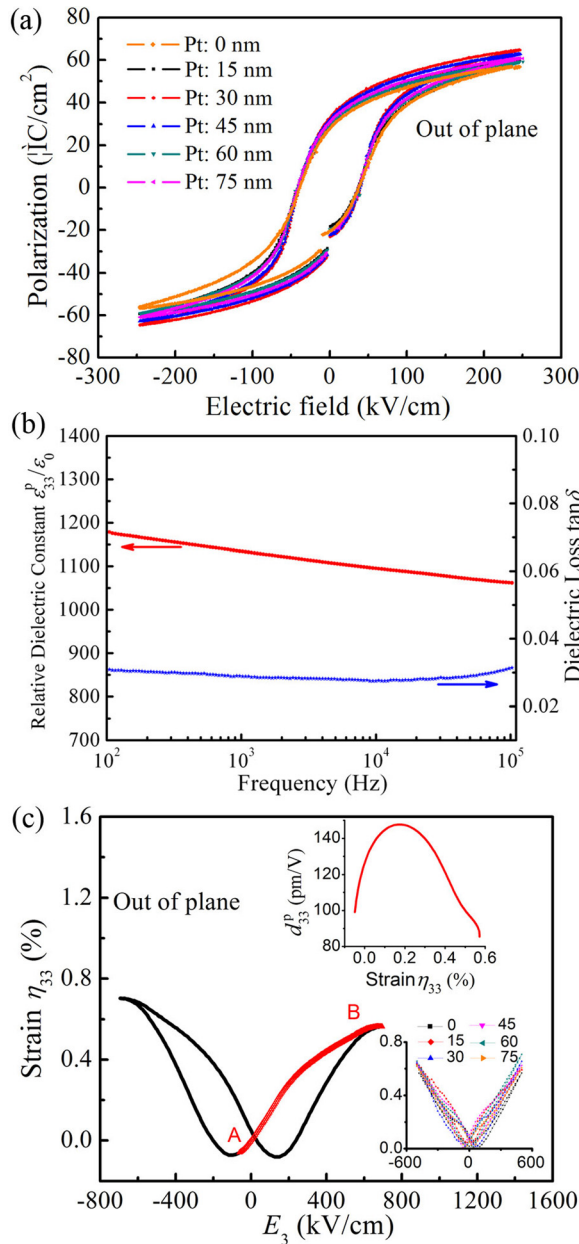


FIG. 2. (a) Ferroelectric hysteresis loops for the PZT films in PZT/Pt/Ni heterostructures with different thickness of Pt buffer layers. (b) Dielectric properties and (c) out-of-plane piezoelectric strain  $\eta_{33}$  of the PZT film; the top inset curve in (c) is the piezoelectric coefficient  $d_{33}^p$  as function of strain  $\eta_{33}$  extracted from AB portion (in red color) of the piezoelectric loop; the bottom inset curves in (c) are the strain  $\eta_{33}$  versus electric field  $E_3$  loops as function of Pt buffer layer thickness.

magnetic fields.<sup>10</sup> Such robust piezomagnetic coupling directly foreshows a large ME voltage output. As seen from Fig. 3(b), the ME voltage coefficient  $\alpha_{E31}$  of all samples is proportional to the piezomagnetic coefficient  $d\lambda/dH_1^{\text{dc}}$  with increasing  $H_1^{\text{dc}}$ . More importantly, Fig. 3(b) clearly indicates that there is an optimum thickness value for the Pt buffer layer that enables a most efficient strain transfer across interfaces, as demonstrated by the largest  $\alpha_{E31}$  of  $772 \text{ mV cm}^{-1} \text{ Oe}^{-1}$  at a moderate Pt thickness of 30 nm, significantly larger than those in quasi-2-2 PZT/CFO, PZT/LaNiO<sub>3</sub>/CFO film heterostructures and quasi-2-2 PZT/LSMO.<sup>10,17,18</sup> Moreover, compared with the relatively large magnetic field (i.e.,  $10^2 \sim 10^3 \text{ Oe}$ ) in the ceramic-based ME

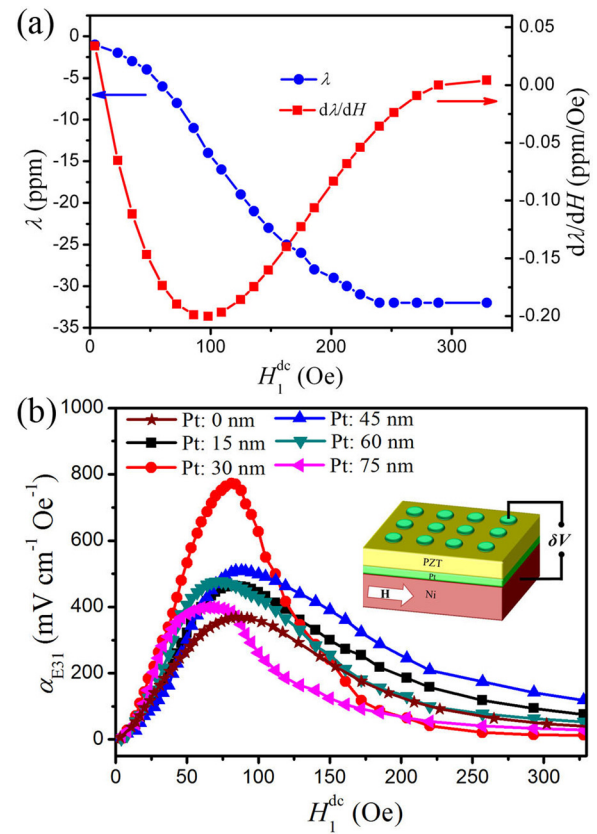


FIG. 3. (a) The in-plane magnetostrictive strain  $\lambda$  and the corresponding piezomagnetic coefficient  $d\lambda/dH$  of the PZT/Pt/Ni heterostructure. (b) The in-plane magnetoelectric (ME) coupling coefficient  $\alpha_{E31}$  for heterostructures with different thicknesses of Pt buffer layer under different magnetic bias  $H_1^{\text{dc}}$ . The inset of (b) shows the schematic illustration on how  $\alpha_{E31}$  was measured.

film heterostructures, the small magnetic field of 86 Oe in present work undoubtedly favored the miniaturization and the energy conservation.

As an interfacial bonding layer, obviously, the Pt buffer layer affects the ME coupling between the PZT film and Ni foil. By considering the interface strain transfer efficiency  $k$ ,<sup>16,17</sup> the ME voltage coefficient  $\alpha_{E31}$  can be estimated by

$$\alpha_{E31} = \frac{-2kd_{31}^p t^m}{(s_{11}^m + s_{12}^m)e_{33}^p kt^p + (s_{11}^p + s_{12}^p)e_{33}^p t^m - 2(d_{31}^p)^2 kt^m} \times \frac{d\lambda}{dH_1^{\text{dc}}}. \quad (1)$$

Here,  $t^m$  and  $t^p$  are the thicknesses of the Ni and PZT layers, respectively;  $s_{ij}^p$  and  $s_{ij}^m$  are elastic compliances of the PZT ( $s_{11}^p = 8.6 \times 10^{-12} \text{ m}^2/\text{N}$ ,  $s_{12}^p = -2.8 \times 10^{-12} \text{ m}^2/\text{N}$ ) and Ni ( $s_{11}^m = 7.3 \times 10^{-12} \text{ m}^2/\text{N}$ ,  $s_{12}^m = -2.7 \times 10^{-12} \text{ m}^2/\text{N}$ ), respectively, taken from literatures;<sup>25-27</sup>  $e_{33}^p$  and  $d_{31}^p$  are the relative dielectric coefficient and piezoelectric coefficient of the PZT film in the present quasi-2-2 PZT/Pt/Ni film heterostructures, which we directly measure and are shown in Figs. 2(b) and 2(c). Given that the small magnitude of the magnetostrictive strain (i.e.,  $-34 \text{ ppm}$  as a maximum, see Fig. 3(a)), it is rational to assume a constant  $d_{33}$  of  $100 \text{ pm/V}$  when applying magnetic fields to the film heterostructures, as seen from the inset of Fig. 2(c). Accordingly,  $d_{31}^p$  in Eq. (1) can be

approximated as a constant of  $-50 \text{ pm/V}$  considering  $d_{33} \approx -2d_{31}$ .<sup>28,29</sup> The above analysis for Eq. (1) demonstrates the linear correlation between the ME voltage coefficient  $\alpha_{E31}$  and the piezomagnetic coefficient  $d\lambda/dH_1^{\text{dc}}$ , agreeing well with the experimental observations shown in Fig. 3(b). For illustration, the  $H_1^{\text{dc}}$ -dependent  $\alpha_{E31}$  calculated based on Eq. (1) for the sample with 30 nm Pt layer shows similar variations trends with corresponding experiments, as shown in Fig. 4(a). The calculated  $\alpha_{E31}$  is higher because an ideal 100% strain transfer efficiency  $k$  is assumed, leading to a peak value of  $943 \text{ mV cm}^{-1} \text{ Oe}^{-1}$ .

Equation (1) also allows us to identify the actual strain transfer efficiency  $k$ , with known experimental values of  $d\lambda/dH_1^{\text{dc}}$  and  $\alpha_{E31}$  under a given magnetic field (e.g., see Fig. 4(a)). For further illustration, Fig. 4(b) shows the actual strain transfer efficiency  $k$  as function of the thickness of the Pt buffer layer, with corresponding peak values of  $\alpha_{E31}$  shown for comparison. As seen, the sample with 30-nm-thick Pt buffer layer shows the largest  $\alpha_{E31}$  of  $772 \text{ mV cm}^{-1} \text{ Oe}^{-1}$ , resulting from the optimum interface strain transfer efficiency of 83%. As we know, the Pt film serves as a buffer layer to release the stress from the Ni foil and hence improves the film quality of PZT. However, on the other hand, as an inert layer, the Pt film also inhibits the efficient stress transfer during the magnetic-mechanic-electric ME

coupling. So, a peak value of  $\alpha_{E31}$  was observed in the PZT/Pt/Ni film heterostructure with a Pt-thickness of 30 nm.

In summary, polycrystalline quasi-2-2 multiferroic PZT/Pt/Ni film heterostructures have been prepared by sol-gel spin-coating method. Pt films of different thicknesses have been introduced to relieve the structural mismatch between the bottom Ni foil and top PZT film and to help crystallize the PZT, aimed at improving the interface quality and hence the direct ME coupling. At the optimized Pt-thickness of 30 nm, such polycrystalline quasi-2-2 film heterostructures exhibit a giant ME voltage coefficient  $\alpha_{E31}$  of  $772 \text{ mV cm}^{-1} \text{ Oe}^{-1}$  at a low dc magnetic bias field of 86 Oe, with a corresponding strain transfer efficiency  $k$  of 83% obtained by combined experimental and theoretical analysis. This high strain transfer efficiency is comparable to that in epitaxial quasi-2-2 multiferroic film heterostructures.

This work was supported by the NSF of China (Grant Nos. 51332001, 11234005, 51221291, 21201078, and 51472140), Beijing Education Committee (Grant No. 20121000301), and the NSF (Grant Nos. DMR-1410714, DMR-0820404, and DMR-1210588).

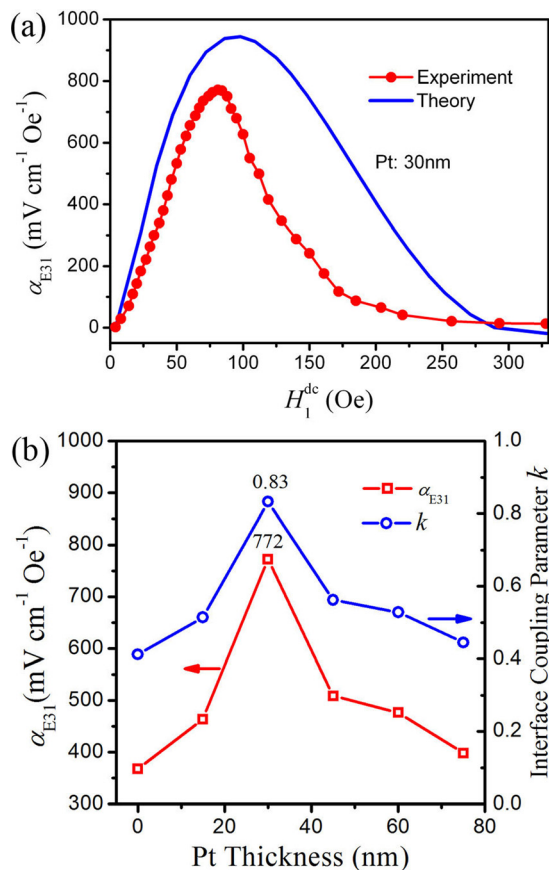


FIG. 4. (a) Experimentally measured ME coupling coefficient  $\alpha_{E31}$  for PZT/Pt/Ni film heterostructure with 30 nm Pt buffer layer, compared with calculated value from the theoretical model in Eq. (1). (b) Measured maximal  $\alpha_{E31}$  as function of Pt thickness and the corresponding interfacial coupling parameter  $k$  calculated from Eq. (1).

- <sup>1</sup>C. C. W. Nan, M. I. Bichurin, S. X. Dong, D. Viehland, and G. Srinivasan, *J. Appl. Phys.* **103**, 031101 (2008).
- <sup>2</sup>J. Ma, J. M. Hu, Z. Li, and C. W. Nan, *Adv. Mater.* **23**, 1062 (2011).
- <sup>3</sup>P. Martins and S. Lanceros-Méndez, *Adv. Funct. Mater.* **23**, 3371 (2013).
- <sup>4</sup>T. Nan, Y. Hui, M. Rinaldi, and N. X. Sun, *Sci. Rep.* **3**, 1985 (2013).
- <sup>5</sup>E. Lage, C. Kirchhof, V. Hrkac, L. Kienle, R. Jahns, R. Knochel, E. Quandt, and D. Meyners, *Nat. Mater.* **11**, 523 (2012).
- <sup>6</sup>C. Israel, N. D. Mathur, and J. F. Scott, *Nat. Mater.* **7**, 93 (2008).
- <sup>7</sup>J. Zhai, Z. Xing, S. Dong, J. Li, and D. Viehland, *Appl. Phys. Lett.* **88**, 062510 (2006).
- <sup>8</sup>Y. Zhang, Z. Li, C. Deng, J. Ma, Y. Lin, and C.-W. Nan, *Appl. Phys. Lett.* **92**, 152510 (2008).
- <sup>9</sup>S. Dong, J. Zhai, J. F. Li, D. Viehland, and S. Priya, *Appl. Phys. Lett.* **93**, 103511 (2008).
- <sup>10</sup>J. P. Zhou, H. C. He, Z. Shi, G. Liu, and C. W. Nan, *J. Appl. Phys.* **100**, 094106 (2006).
- <sup>11</sup>H. Greve, E. Woltermann, H.-J. Quenzer, B. Wagner, and E. Quandt, *Appl. Phys. Lett.* **96**, 182501 (2010).
- <sup>12</sup>Z. H. Tang, M. H. Tang, X. S. Lv, H. Q. Cai, Y. G. Xiao, C. P. Cheng, Y. C. Zhou, and J. He, *J. Appl. Phys.* **113**, 164106 (2013).
- <sup>13</sup>R. Jahns, A. Piorra, E. Lage, C. Kirchhof, D. Meyners, J. Gugat, M. Krantz, M. Gerken, R. Knöchel, and E. Quandt, *J. Am. Ceram. Soc.* **96**, 1673 (2013).
- <sup>14</sup>R. C. Kambale, J. Ryu, D. Patil, Y. S. Chai, K. H. Kim, W.-H. Yoon, D.-Y. Jeong, D.-S. Park, J.-W. Kim, J.-J. Choi, and C.-W. Ahn, *J. Phys. D: Appl. Phys.* **46**, 092002 (2013).
- <sup>15</sup>T. Wu, M. A. Zurbuchen, S. Saha, R. V. Wang, S. K. Streiffer, and J. F. Mitchell, *Phys. Rev. B* **73**, 134416 (2006).
- <sup>16</sup>M. I. Bichurin and V. M. Petrov, *Phys. Rev. B* **68**, 054402 (2003).
- <sup>17</sup>J. Wang, L. Wang, G. Liu, Z. Shen, Y. Lin, and C. W. Nan, *J. Am. Ceram. Soc.* **92**, 2654 (2009).
- <sup>18</sup>J. Wang, Z. Li, Y. Shen, Y. Lin, and C. W. Nan, *J. Mater. Sci.* **48**, 1021 (2013).
- <sup>19</sup>W. Z. Liang, Z. Li, Z. X. Bi, T. X. Nan, H. Du, C. W. Nan, C. L. Chen, Q. X. Jia, and Y. Lin, *J. Mater. Chem. C* **2**, 708 (2014).
- <sup>20</sup>D. J. Wouters, G. J. Norga, and H. E. Maes, *Mater. Res. Soc. Symp. Proc.* **541**, 381 (1998).
- <sup>21</sup>J. F. M. Cillessen, M. W. J. Prins, and R. M. Wolf, *J. Appl. Phys.* **81**, 2777 (1997).
- <sup>22</sup>C. H. Lin, P. A. Friddle, C. H. Ma, A. Daga, and H. Chen, *J. Appl. Phys.* **90**, 1509 (2001).
- <sup>23</sup>Y. Wang, C. Ganpule, B. T. Liu, H. Li, K. Mori, B. Hill, M. Wutting, R. Ramesh, J. Finder, Z. Yu *et al.*, *Appl. Phys. Lett.* **80**, 97 (2002).
- <sup>24</sup>Y. Cao, G. Sheng, J. X. Zhang, S. Choudhury, Y. L. Li, C. Randall, and L.-Q. Chen, *Appl. Phys. Lett.* **97**, 252904 (2010).

- <sup>25</sup>N. Pertsev, V. Kukhar, H. Kohlstedt, and R. Waser, *Phys. Rev. B* **67**, 054107 (2003).
- <sup>26</sup>J. J. Wang, J.-M. Hu, L.-Q. Chen, and C.-W. Nan, *Appl. Phys. Lett.* **103**, 142413 (2013).

<sup>27</sup>D. Sander, *Rep. Prog. Phys.* **62**, 809 (1999).

<sup>28</sup>I. L. Guy, S. Muensit, and E. M. Goldys, *Appl. Phys. Lett.* **75**, 4133 (1999).

<sup>29</sup>D. Berlincourt, H. Jaffe, and L. R. Shiozawa, *Phys. Rev.* **129**, 1009 (1963).